Materials Horizons

ROYAL SOCIETY OF CHEMISTRY

COMMUNICATION

View Article Online
View Journal | View Issue

Cite this: *Mater. Horiz.*, 2021, 8, 2057

Received 18th March 2021,
Accepted 11th May 2021

DOI: 10.1039/d1mh00461a

rsc.li/materials-horizons

A highly transparent ionogel with strength enhancement ability for robust bonding in an aquatic environment†

Zhenchuan Yu[ab] and Peiyi Wu *[ab]

An underwater adhesive with strong, fast and stable adhesion ability has become an urgent requirement for various industrial applications. Herein, a highly transparent ionogel based on a fluorine-rich poly(ionic liquid) and the corresponding ionic liquid monomer has been developed and used as an underwater adhesive. Strong and stable underwater adhesion can be realized by taking advantage of the excellent interface adaptability and high mechanical strength of this ionogel. The underwater adhesion strength could reach as high as 5.18 ± 0.27 MPa. In addition, it can also realize robust bonding over a wide pH range (0–14). A waterproof transparent tape based on the ionogel has also been developed and it can carry out repair work in wet and aquatic environments.

New concepts

Underwater adhesives are highly desirable and indispensable materials in many fields. However, achieving strong adhesion in an aquatic environment remains an enormous challenge due to the effect of water molecules, which can form a hydrated film to prevent contact between the adhesive and substrate in the aquatic environment. Though several underwater adhesives based on catechol groups, host–guest chemistry, electrostatic and hydrophobic interactions have been designed, they still suffer from pH sensitivity and instability. More importantly, limited by their poor mechanical properties, the underwater adhesion strength of those adhesives is usually rather weak (<1 MPa). Herein, a fluorine-rich ionogel with a strength enhancement ability based on a poly(ionic liquid) and a corresponding ionic liquid monomer has been developed. This ionogel can eliminate the interference of water molecules and achieve adhesion in an aquatic environment. In addition, the modulus of the ionogel can be greatly improved by *in situ* polymerization of ionic liquid monomers. Taking advantage of the excellent interface compatibility and high mechanical strength of the ionogel, its underwater adhesion strength could reach as high as 5.18 ± 0.27 MPa. A waterproof transparent tape based on this ionogel has been developed, and it can carry out repair work in wet and aquatic environments. It is believed that this work may provide a novel strategy for fabricating underwater adhesives with multifunctionality and adaptability for various environmental conditions.

1. Introduction

Underwater adhesives are indispensable material in many fields, such as underwater repair, water-based devices, medical surgery, wound dressings, and stretchable electronics. However, developing an underwater adhesive with a strong, fast and stable bonding capability remains an enormous challenge. Due to the influence of water molecules, which can form a hydrated water film on the surface of the substrate to prevent contact between the adhesive and substrate, the adhesion strength is greatly decreased or even eliminated in an aquatic environment.[1–3] In order to break down the hydrated water film, several strategies based on catechol groups,[4–7] host–guest chemistry,[8] electrostatic-[9,10] and hydrophobic-interactions[11–13] have been used to design underwater adhesives. However, they often suffer from the problems of being susceptible to oxidation, pH sensitivity, the need for modifying the surface of the substrate in advance, and organic solvent leakage. More importantly, limited by their poor mechanical properties, the underwater adhesion strength of those adhesives is usually weak (<1 MPa).

In general, in order to obtain robust bonding, the adhesive material should have a high mechanical strength and must be in full contact with the surface of the substrate to achieve a strong interface interaction.[10,14–16] However, materials with high mechanical strength are usually difficult to adapt to rough substrate surfaces, resulting in weak interface interactions. Strong bonding can be achieved by the *in situ* formation of a tough hydrogel on the surface of the substrate and linking it to the substrate by covalent bonding.[17] However, the surface of

[a] *State Key Laboratory for Modification of Chemical Fibers and Polymer Materials, College of Chemistry, Chemical Engineering and Biotechnology, Center for Advanced Low-Dimension Materials, Donghua University, Shanghai 201620, P. R. China. E-mail: wupeiyi@dhu.edu.cn*

[b] *State Key Laboratory of Molecular Engineering of Polymers, Department of Macromolecular Science and Laboratory of Advanced Materials, Fudan University, Shanghai 200433, P. R. China. E-mail: peiyiwu@fudan.edu.cn*

† Electronic supplementary information (ESI) available. See DOI: 10.1039/d1mh00461a

the substrate needs to be modified in advance and this strategy is not suitable for a water environment. All in all, a strategy that can not only effectively destroy the hydrated water layers but also break the contradiction between mechanical strength and interface adaptability is the key to establishing robust bonding in an aquatic environment.

It is well known that fluoropolymers display hydrophobicity, and high thermal and chemical resistance due to their small van der Waals radius, low polarizability, the strong electronegativity of the fluorine atom and the strong C–F bond.[18–21] Herein, taking advantage of the fact that fluoropolymers can eliminate the interference of water molecules,[22–24] an ionogel (IG) based on a fluorine-rich poly(ionic liquid), poly[MATAC][TFSI], termed PIL, and a corresponding ionic liquid monomer, [MATAC][TFSI], termed IL, has been developed and used as an underwater adhesive. The water molecules can form a hydrated film on the substrate surface in an aquatic environment (Fig. 1a(i)). When the IG was pressed onto the substrate, the hydrated film was broken and the IG could fully conform to the rough substrate surfaces due to its hydrophobic property and low mechanical strength (Fig. 1a(ii)). However, the loose polymer chains of the ionic gel cannot form high-density interactions with the substrate surface. In addition, the mechanical strength of the IG is too low to sustain sufficient load during the debonding process, and therefore robust underwater bonding cannot be achieved. When the IG was exposed to UV light, the ionic liquid monomer ([MATAC][TFSI]) inside the IG could be further polymerized and more polymer chains can be formed (the IG after polymerization of the ionic liquid monomers is termed pIG). On one hand, the high-density polymer chains at the IG surface provide more noncovalent bonding sites with the substrate surfaces (Fig. 1a(iii)). On the other hand, the dramatic increase in the IG modulus allows it to withstand high shear stresses during the debonding process. As a result, strong and stable underwater adhesion can be realized by taking advantage of the excellent interface compatibility and high mechanical strength of the ionogel. The underwater adhesion strength is as high as 5.18 ± 0.27 MPa, which is one or two orders of magnitude higher than most reports in the literature. Moreover, the IGs possess a wide range of environmental adaptability and can function in strong salt (1 M NaCl), alkali (1 M NaOH) and acid (1 M HCl) solutions.

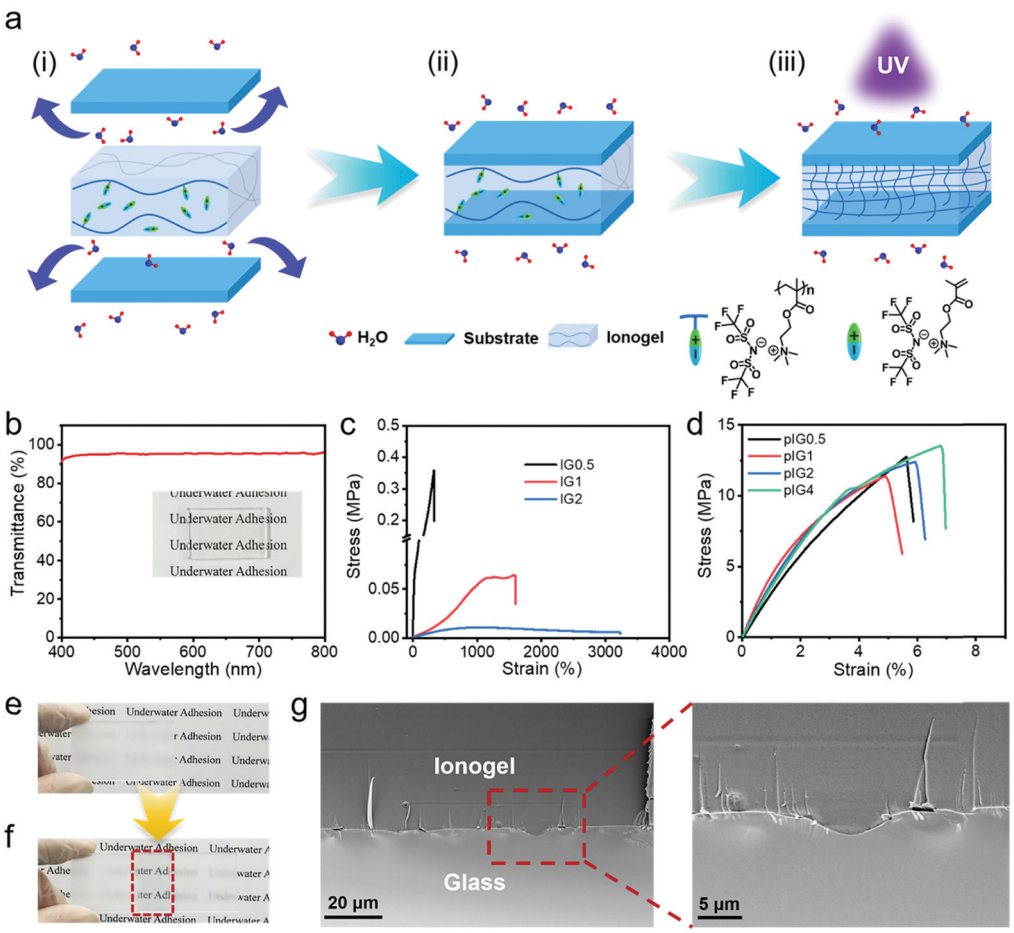

Fig. 1 (a) Schematic diagram of the IGs adhered to the substrate and polymerized *in situ* to form strong adhesion in an aquatic environment. (b) The transmittance of IG0.5 in the visible wavelength range. Inset: Photograph of IG0.5. (c) True stress–strain curves of the IGs. (d) True stress–strain curves of the pIGs. (e) Photo of polished glass. (f) Photo of polished glass after being bonded with IG2, and the bonding area becomes transparent. (g) SEM microscopy image of the bonding interface between glass and pIG2.

A waterproof transparent tape based on the ionogel has also been developed and it can carry out repair work in wet and aquatic environments.

2. Results and discussion

The underwater adhesive ionogels were prepared using a fluorine-rich PIL as the polymer network and a corresponding monomer as the solvent through the solvent-casting method. A series of ionogels with PIL : IL weight ratios of 1 : 0.5, 1 : 1, 1 : 2 and 1 : 4 were prepared, termed IG0.5, IG1, IG2 and IG4, respectively. The IGs after polymerization of the ionic liquid monomers were termed pIG0.5, pIG1, pIG2 and pIG4, respectively. Due to the excellent compatibility between the PIL and IL, the IGs are fully transparent and the average transmittance can reach 95.2% in the visible light range (Fig. 1b). Owing to the large dipole moment of the C–F bond and the Coulomb potential between the PIL and IL, ion–dipole and ion–ion interactions can be established in the IGs and provide intrinsic tensile properties for the ionogel.[22–24] The true stress–strain curves of the IGs are shown in Fig. 1c. The Young's modulus and strain at break of IG0.5 are 1.05 MPa and 330%, respectively. With the increase in IL content, more soft ion domains with a low energy barrier were formed inside the IGs and the modulus of the IGs decreased significantly. For example, the Young's modulus of IG2 decreased to 9.77 kPa; meanwhile, the strain at break of IG2 increased from 330 to 3230%. As the ratio of PIL and IL increases to 1 : 4, the IG4 is so soft that its stress–strain curve cannot be measured by the tensile machine. Corresponding rheological results of the IGs are shown in Fig. S1 (ESI†). The modulus of the IGs decreased significantly with the increase of IL content, indicating that the mechanical properties of the ionogels can be easily tuned by changing the ratio of PIL to IL. More importantly, the IGs contain an IL monomer, which provides the possibility for further modification of the mechanical properties after the IGs have been formed. As shown in Fig. 1d, the Young's modulus of the pIGs increased by two–five orders of magnitude over the IGs and could reach up to ~400 MPa, which demonstrates that the ionogels are able to make the transition from "soft" to "tough". The disappearance of the C=C stretching vibration band of the IGs (1638 cm^{-1}) proved that polymerization had been carried out (Fig. S2, ESI†). The transition in mechanical properties may be attributed to the disappearance of the soft ion domain of the ionic liquid monomer and the newly formed polymer chains entangled with the PIL chains. In addition, the ability of the ionogels to transform their mechanical properties can break the contradictions between the mechanical strength and interface adaptability, making it possible to achieve robust bonding. On the one hand, the IGs could fully contact with the surface of the substrate, and a topological structure can be formed between the IGs and the substrate due to the low modulus of the IGs. On the other hand, after the IL monomer had been polymerized, more polymer chains were formed, which provided more interface interactions between the polymer network and solid surfaces, and the tough pIGs can withstand high shear stresses during the debonding process.

In order to prove the excellent interface adaptability of the IGs, a series of experiments was carried out. After polishing

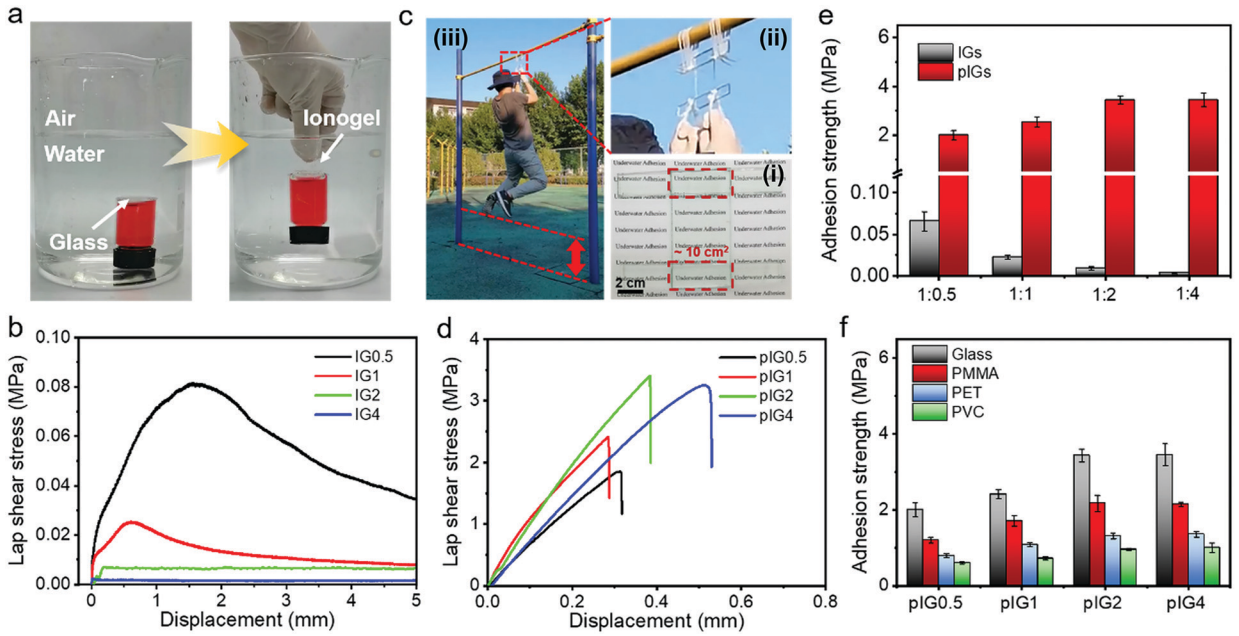

Fig. 2 (a) Digital picture of glass bonded with IG0.5 in an aquatic environment. (b) Lap shear curves of IGs in the bonding of glass in an aquatic environment. (c) Digital pictures of glass, which was bonded with IG0.5 and further *in situ* polymerized under UV light. The adhesion area is ~10 cm^2 (i). The bonded glasses can withstand the weight of an adult (~68 kg) and the pulling up and down of the body (ii and iii). (d) Lap shear curves of the pIGs bonding with glass in an aquatic environment. (e) Underwater adhesion strength of the IGs and pIGs with different weight ratios of PIL and IL. (f) Underwater adhesion strength of the pIGs with different substrates.

with sandpaper, the surface of glass becomes rough, and the transparent glass becomes translucent due to the highly reflective ability of the rough surface (Fig. 1e). However, after the glass is bonded with IG2, the rough glass surface is filled with the ionogel and the bonded area (in the red box in Fig. 1f) becomes transparent, which means that the IGs are well adapted to rough surfaces. The change in transmittance of the glass also proved this (Fig. S3, ESI†). The glass is highly transparent and the average transmittance could reach up to 91.5% in the visible wavelength range. Moreover, the average transmittance decreased to 81.5% after the glass was polished with sandpaper. However, the average transmittance recovered to 89.5% after bonding with the IGs. The slight decrease in transmittance compared with the original value is probably due to the increase of glass thickness. The scanning electron microscopy (SEM) image of the bonded glass is shown in Fig. 1g. The mechanical interlocking structure can be observed at the interface and there are no gaps remaining, indicating that the ionogel has excellent interface adaptability and can be well adapted to the rough surfaces of substrates.

The underwater adhesion properties of the ionogel were characterized. As shown in Fig. 2a and Movie S1 (ESI†), IG0.5 can rapidly adhere to glass, polypropylene (PP), polytetrafluoroethylene (PTFE) and iron (Fe), demonstrating the underwater adhesion ability of the ionogels. The underwater adhesion process of the ionogel includes two steps. First, due to its hydrophobicity, the ionogel can eliminate the interference of water molecules and break the hydrated film on the substrate surface. Second, as shown in Fig. S4 (ESI†), the abundant functional groups inside the ionogel can form various interactions with different groups, including ion–dipole interactions,[23,25] dipole–dipole interactions,[26–28] metal complexation,[29,30] electrostatic interactions,[9,31] cation–π interactions[9] and van der Waals interactions.[32] As a result, underwater bonding can be formed. It is noteworthy that the ionogel is almost invisible in an aquatic environment, which is desirable in practical applications. The adhesion strength of the IGs was characterized by the lap shear test method (Fig. 2b). According to the lap shear curve, the underwater adhesion strength of IG0.5 can reach 0.08 MPa. With the increase in IL content, the underwater adhesion strength decreased significantly, which was due to the rapid decrease of the mechanical strength. It is worth noting that the underwater adhesion strength of IG0.5 is still less than 0.1 MPa although it has the best underwater adhesion ability among the IGs. The low adhesion strength is mainly limited by the low mechanical strength of the IGs. Fortunately, the mechanical strength of the ionogels can be tuned by polymerization of the IL monomer (Fig. 1d). As a result, the underwater adhesion strength can be greatly improved. For instance, the glasses were bonded with IG0.5 with an adhesion area of $\sim$10 cm^2 in an aquatic environment and the IL monomer was polymerized *in situ* under UV light. The glasses can bear the weight of an adult ($\sim$68 kg) and allow the adult to move up and down (Fig. 2c and Movie S2, ESI†), which indicates that pIG0.5 has strong adhesion properties. The lap shear curve and underwater adhesion strength of the pIGs are shown in Fig. 2d and e, respectively. The underwater adhesion strength of pIG0.5 increases dramatically and reaches 2.0 $\pm$ 0.19 MPa, which is two orders of magnitude higher than that before polymerization. The underwater adhesion strength can be further increased to 3.43 $\pm$ 0.17 MPa with an increase in the PIL and IL ratio to 1 : 2. The increase of adhesion strength may be because IG2 has a lower modulus than IG0.5 and therefore IG2 has a higher interfacial adaptability before polymerization. As IG0.5 and IG2 have similar modulus values after *in situ* polymerization (Fig. 1d), better interface adaptability results in more interface interactions and is more favorable for adhesion. The underwater adhesion strength of pIG4 (3.45 $\pm$ 0.28 MPa) is similar to that of pIG2, which may be because pIG2 has been able to accommodate rough interfaces adequately. In short, the excellent interface adaptability before polymerization and strong mechanical strength after polymerization of the ionogel endow it with super adhesive ability. The underwater adhesion ability of the pIGs with different materials was also studied. As shown in Fig. 2f, the underwater adhesion strength for polymethyl methacrylate (PMMA), polyethylene terephthalate (PET), and polyvinyl chloride (PVC) could reach 2.17 $\pm$ 0.21, 1.31 $\pm$ 0.07 and 0.94 $\pm$ 0.03 MPa, indicating that ionogels have an outstanding adhesion ability with different materials. The difference in adhesion strength may be due to the different polarity of the materials.

It has been proved that deformation of the adhesive could consume a large amount of mechanical energy when the adhesive is detached from a solid, which can significantly increase the adhesion strength.[17,33–35] In order to increase the energy dissipation during the peeling process, an ionic liquid, $[N_{4111}][TFSI]$, which cannot be polymerized, was introduced into the ionogel. The ionogels with PIL : IL : $[N_{4111}][TFSI]$ weight ratios of 1 : 2 : 0.2, 1 : 2 : 0.4, 1 : 2 : 0.6 and 1 : 2 : 0.8 were termed IG2-N0.2, IG2-N0.4, IG2-N0.6 and IG2-N0.8, respectively. In addition, the IG2-N samples after polymerization of the ionic liquid monomers were termed pIG2-N0.2, pIG2-N0.4, pIG2-N0.6 and pIG2-N0.8, respectively. As shown in Fig. 3a, with the increase in $[N_{4111}][TFSI]$ content, the strain at break increased clearly because of the plasticizing effect. For instance, with the mass ratio of $[N_{4111}][TFSI]$ increased from 1 : 2 to 1 : 2 : 0.4, the strain at break of the ionogel increased from 6% to 173% accompanied by a slight decrease in Young's modulus (from 375 MPa to 242 MPa). The stress–strain curves cyclic tensile test is shown in Fig. S5 (ESI†). The tensile curves show significant hysteresis, indicating effective energy dissipation during the stretching process. The recovery rate, defined as the ratio of the second hysteresis loop to the first hysteresis loop,[36] is 58.9%, which means that more than 40% of the energy was dissipated in the process of stretching. Due to the energy dissipation, the underwater adhesion strength of the pIG2-N samples increased significantly with the addition of $[N_{4111}][TFSI]$. As shown in Fig. 3b and c, the underwater adhesion strength of the pIG2-N samples for glass increased from 3.44 $\pm$ 0.17 MPa to 5.18 $\pm$ 0.27 MPa with the weight ratio of $[N_{4111}][TFSI]$ increased from 0 to 0.4. Similarly, the underwater adhesion strength for PMMA, PET and PVC also increased to 4.50 $\pm$ 0.14 MPa, 1.93 $\pm$ 0.08 MPa and 1.38 $\pm$ 0.11 MPa. However, with a further

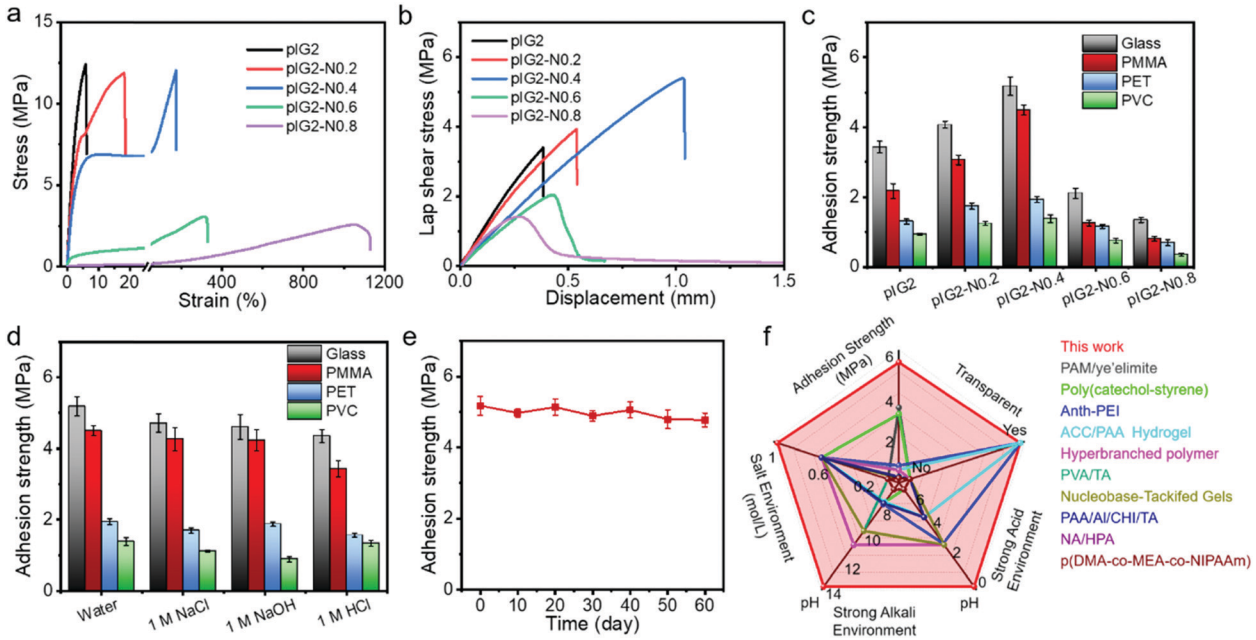

Fig. 3 (a) True stress–strain curves of the pIG2-N samples. (b) Lap shear curves of the pIG2-N samples for glass. (c) Underwater adhesion strength of the pIG2-N samples for different materials. (d) Underwater adhesion strength of pIG2-N0.4 for different materials in different solutions. (e) Long-term stability of the adhesion strength of pIG2-N0.4 in an aquatic environment. (f) Comparison of the underwater adhesion properties of pIG2-N samples and adhesives reported in the literature.

increase in the IL proportion, the underwater adhesion strength decreased rapidly. For example, the underwater adhesion strength of pIG2-N0.6 for glass decreased to 2.10 ± 0.14 MPa. Due to the drastic decrease in the modulus of the ionogel, pIG2-N0.6 cannot withstand shear stress during the debonding process, resulting in a dramatic reduction in the underwater adhesion strength. It is worth noting that the adhesion strength of pIG2-N0.4 for glass in the aquatic environment is similar to that in air (Fig. S6, ESI†), indicating that water molecules have no effect on the adhesion properties of the ionogel.

It has been demonstrated that cationic groups can exclude salt ions from the surface of the substrate, which makes it possible for ionogels to maintain their adhesion properties in salt solutions.[3] As shown in Fig. 3d, the underwater adhesion strength is still 4.71 ± 0.26 MPa in 1 M NaCl solution, which means that the ionogel can resist interference from the salt ions. As it is well known that fluoropolymers show outstanding chemical resistance due to the their polarizability, small van der Waals radius, strong electronegativity, and strong C–F bond of the fluorine atoms, the environmental adaptability of the ionogel was also studied. As shown in Fig. 3d, there is no significant decrease in the underwater adhesion strength of pIG2-N0.4 in strong alkali (1 M NaOH) and acid (1 M HCl) solution, and the underwater adhesion strength remains at 4.60 ± 0.35 MPa and 4.35 ± 0.18 MPa. The pIG2-N0.4 also has a strong adhesion strength in acid, alkali and salt solution for PMMA, PET and PVC, which proves that the ionogel has excellent environmental adaptability. The long-term stability of pIG2-N0.4 was also studied (Fig. 3e). The adhesion strength for glass in an aquatic environment can be maintained 4.77 ± 0.20 MPa after soaking in water for 60 days, indicating that the ionogel can withstand long-term immersion under water. The underwater adhesion strengths of various adhesives reported in the literature are summarized in Fig. 3f.[4,6,11,14,37–42] The ionogel in this work shows a much higher underwater adhesion strength and wider pH adaptation. Meanwhile, the ionogel also has the advantages of transparency, fast adhesion (in 5 min) and long-term stability (>60 days). We believe that the unparalleled underwater adhesion properties give this ionogel the prospect of very broad application.

Transparent tapes have a wide range of applications in daily life. However, commercial transparent tapes usually lose their adhesion ability in an aquatic environment due to the influence of water molecules. In this paper, a waterproof transparent tape (WTT) has been developed taking advantage of the transparency and superb adhesion ability of the ionogel. The WTT was fabricated by simply coating the IG2-N0.4 onto the surface of a commercial PET film. Because of the simple fabrication process, WTT can be prepared on a large scale. As shown in Fig. 4a, a flexible WTT with a size of 20 × 20 cm was prepared. It is worth noting that the PET film can retain its intrinsic transparency after coating with the IG2-N0.4 due to the high light transmission of the IG2-N0.4. As shown in Fig. 4b, the average transmittance of the WTT can reach 93.12% in the visible-light range, which is almost the same as that of the commercial PET film (93.72%). The adhesion properties of the WTT in a wet environment were characterized. As shown in Fig. S7a and Movie S3 (ESI†), commercial transparent tapes cannot stop a rubber balloon from

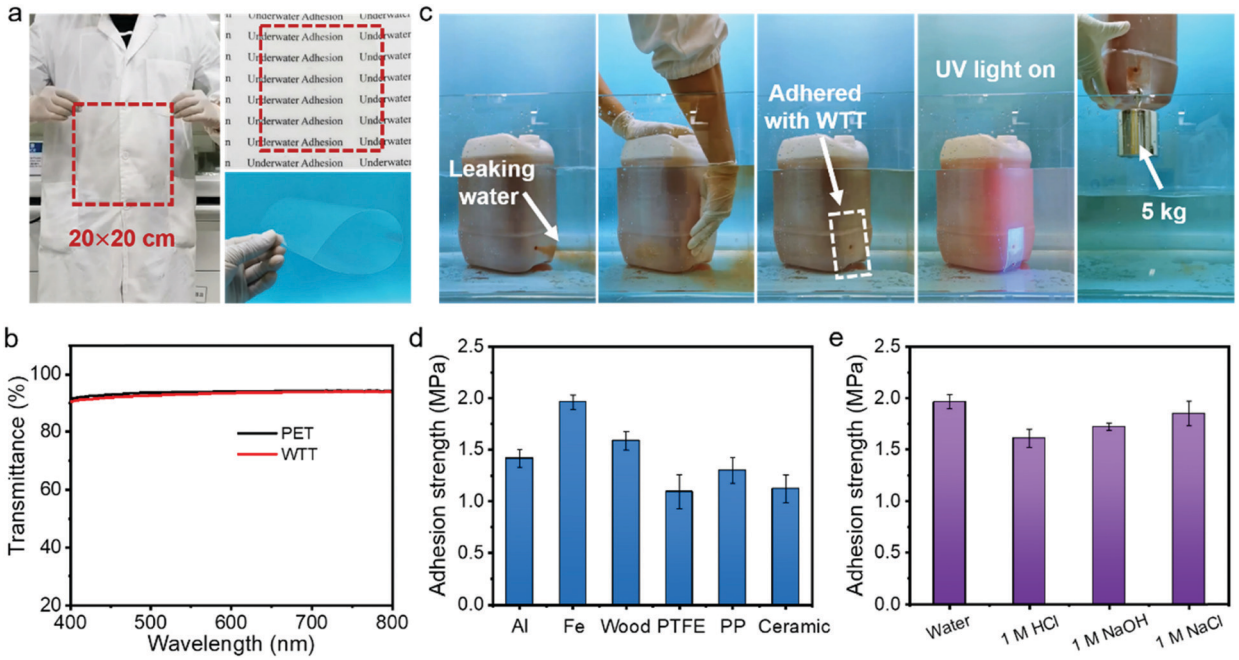

Fig. 4 (a) Photographs of the waterproof transparent tape with a size of 20 × 20 cm. (b) Transmittance of PET and waterproof transparent tape in the visible wavelength range. (c) Photographs showing the ability of the waterproof transparent tape to repair the hole in a bucket in an aquatic environment. (d) Underwater adhesion strength of the waterproof transparent tape for different materials. (e) Adhesion strength of the waterproof transparent tape with Fe in different environments.

leaking water. However, the WTT can effectively adhere to the rubber balloon without being affected by the wet environment and the rushing current (Fig. S7b and Movie S4, ESI†). Even if the pressure inside the balloon increases, the WTT can also stop the water leakage. As well as in a wet environment, the WTT also has an underwater repair capability (Fig. 4c and Movie S5, ESI†). We made a round hole (diameter = 1 cm) in a polyethylene bucket and immersed it in water. The water (dyed with neutral red) in the polyethylene bucket will leak out if there is no plug. When the WTT is pressed onto the hole, the hole is well sealed and no water flows out again. After *in situ* polymerization under UV light for 5 min, the WTT can adhere to the surface of the polyethylene bucket firmly and lift a weight of 5 kg, indicating that the WTT can achieve strong bonding with the substrate. The underwater adhesion strengths of the WTT with different materials in an aquatic environment were characterized. As shown in Fig. 4d, the underwater adhesion strengths of WTT with Al, Fe, wood, PTFE, PP and ceramics are 1.42 ± 0.09, 1.96 ± 0.07, 1.59 ± 0.09, 1.09 ± 0.17, 1.30 ± 0.12 and 1.12 ± 0.13 MPa, respectively. In addition, the WTT can maintain strong adhesion in strong acid, base and salt solution, and the adhesion strengths for Fe are 1.61 ± 0.09, 1.72 ± 0.04 and 1.85 ± 0.12 MPa, respectively (Fig. 4e). This result demonstrated that the WTT has the ability to carry out underwater repair work in various harsh environments. The WTT also shows an adhesion ability with biological tissues. As shown in Fig. S8a (ESI†), the WTT can easily adhere to the organs of animals, such as skin, muscle, kidney, and heart. In addition, the WTT can also eliminate the influence of water molecules and achieve adhesion to animal organs in an aquatic environment (Fig. S8b, ESI†). Notably, due to its high light transmission, the WTT is almost visually invisible, both in air and underwater, which is very beneficial for practical applications. The adhesion strength of the WTT to porcine skin in different environments was also characterized. As shown in Fig. S8c (ESI†), the adhesion strength of the WTT to porcine skin is greater than 0.15 MPa, regardless of whether it is in an aquatic environment or in strong acid, alkali, or salt solution. The adhesion properties of the WTT to biological tissues also offer the possibility of its application in medicine.

3. Conclusions

In this work, a fluorine-rich ionogel based on a poly(ionic liquid) and a corresponding ionic liquid monomer has been developed. Due to the hydrophobic property of the ionogel, it can eliminate the interference of water molecules and makes full contact with the substrate in aquatic environments. After *in situ* polymerization of the ionic liquid monomers, the mechanical strength of the ionogel is greatly improved and forms robust adhesion. The underwater adhesion strength can reach 5.18 ± 0.27 MPa, which is much higher than other reports in the literature. Furthermore, the ionogel could maintain strong adhesion in 1 M HCl, NaOH and NaCl solutions. A flexible waterproof transparent tape based on the ionogel has also been developed and it can be used to carry out repair work in wet and aquatic environments. This novel adhesive ionogel has wide application prospects in the field of water-based equipment, underwater transfer, and underwater soft robots.

4. Materials and methods

4.1. Materials

Bistrifluoromethanesulfonimide lithium salt (LiTFSI), 2,2-diethoxyacetophenone, methacryloxyethyltrimethyl ammonium chloride (MATAC) solution (75 wt% in water) and 2,2-azobis (2-methylpropionamidine)dihydrochloride (AIBA) were purchased from Sigma-Aldrich. Butyltrimethylammonium chloride ($[N_{4111}]Cl$) was purchased from Energy Chemical. All other chemicals were purchased from Sinopharm Chemical Reagent Co. All reagents were used without further purification.

4.2. Preparation of the ionic liquid

MATAC and LiTFSI were used to prepare the ionic liquid monomer, [MATAC][TFSI]. 1 mol L^{-1} MATAC solution was mixed with the same volume of 1 mol L^{-1} LiTFSI solution and stirred for 2 hours. The lower oil layer was collected after phase separation had occurred and was washed with deionized water 5 times. After vacuum drying at 70 °C for 12 hours, the transparent ionic liquid monomer, [MATAC][TFSI], was obtained. The ionic liquid, $[N_{4111}][TFSI]$, was prepared using the same method except that MATAC was replaced by $[N_{4111}]Cl$.

4.3. Preparation of the poly(ionic liquid)

The preparation method of the poly(ionic liquid), poly[MATAC][TFSI], was the same as that in the literature.[43] Firstly, 20 g MATAC and 0.075 g AIBA were dissolved in 200 mL distilled water. The polymerization reaction was carried out at 70 °C for 6 h under a nitrogen atmosphere. After cooling to room temperature, the solution was dialyzed for a week and freeze dried. Then, 10 g poly(MATAC) (0.0483 mol) was dissolved in 150 mL distilled water. After being mixed with 50 mL LiTFSI solution (1 mol L^{-1}), the Cl^- in poly(MATAC) was exchanged by $TFSI^-$ as a result of the anion exchange reaction and the polymer was precipitated from the aqueous medium. After being filtered, washed with an excess amount of water and freeze-dried, poly[MATAC][TFSI] was obtained.

4.4. Preparation of the ionogel

The underwater adhesive ionogel was prepared from the poly(ionic liquid) (poly[MATAC][TFSI]), ionic liquid monomer ([MATAC][TFSI]) and ionic liquid $[N_{4111}][TFSI]$. Initially, 1 g poly [MATAC][TFSI] and 5 μL photoinitiator, 2,2-diethoxyacetophenone, with different weight ratios of [MATAC][TFSI] and $[N_{4111}][TFSI]$ were added to 10 mL acetonitrile and the solution was stirred at room temperature for 2 days in dark environment. After being dried in 35 °C for 3 days, drying of the composite was continued for 12 hours in a vacuum oven at 50 °C and then the ionogel was obtained.

4.5. Preparation of the waterproof transparent tape

A commercial PET film with a thickness of 0.1 mm used as the substrate for preparation of the waterproof transparent tape. First, PET was polished with 100 mesh sandpaper and washed with acetone, ethanol, and distilled water. Subsequently, the WTT was prepared by coating the ionogel (the mass ratio of poly[MATAC][TFSI], [MATAC][TFSI] and $[N_{4111}][TFSI]$ is 1 : 2 : 0.4) on PET with a scraper and leaving it at room temperature for 2 days. The coating density was about 0.015 g cm^{-2}.

4.6. Measurement of the underwater adhesion strength

Lap shear testing was carried out using a universal mechanical testing machine (SANS-CMT4104) to characterize the adhesive strength. Prior to adhesion, the substrates, such as glass, PET, PMMA, and PVC, were polished with 100 mesh sandpaper and washed with acetone, ethanol, and distilled water. Subsequently, the IG or IG2-N samples were coated on a substrate and overlapped with another substrate with a bonding area of 15 mm × 10 mm in an aquatic environment. After UV irradiation (365 nm, 20 W) for 5 min, the sample was taken from the water and measured immediately using the dynamometer. The crosshead speed was set to 5 mm min^{-1} to obtain the load–displacement curves. The adhesion strength was determined by dividing the maximum tensile force at joint failure by the overlap area. The adhesion strengths in different environments, such as 1 M HCl, 1 M NaCl, 1 M NaOH solutions, were also measured using the same method. For each type of material, 3–5 samples were measured, and averaged data were reported.

4.7. Characterization

The transmittance of the ionogel was tested using a UV-Vis spectrometer (PerkinElmer Lambda 35). FTIR spectra were recorded using a Nicolet 6700 instrument (Thermo Fisher) using the attenuated total reflectance (ATR) method. The FE-SEM images were taken using a Zeiss Ultra 55 microscope. The tensile stress–strain curves of the ionogels were characterized using the universal mechanical test machine (SANS-CMT4104) with a stretching rate of 50 mm min^{-1}. Due to the large deformation of the sample, the true stress (σ) was used instead of the nominal stress (S), which can be calculated based on the assumption that the ionogels are incompressible.

Conflicts of interest

There are no conflicts to declare.

Acknowledgements

This work was supported by the National Natural Science Foundation of China (No. 51733003 and 21674025).

References

1 H. J. Meredith and J. J. Wilker, *Adv. Funct. Mater.*, 2015, **25**, 5057–5065.
2 A. H. Hofman, I. A. van Hees, J. Yang and M. Kamperman, *Adv. Mater.*, 2018, **30**, 1704640.
3 G. P. Maier, M. V. Rapp, J. H. Waite, J. N. Israelachvili and A. Butler, *Science*, 2015, **349**, 628.

4 X. Su, Y. Luo, Z. Tian, Z. Yuan, Y. Han, R. Dong, L. Xu, Y. Feng, X. Liu and J. Huang, *Mater. Horiz.*, 2020, **7**, 2651–2661.
5 Q. Zhao, D. W. Lee, B. K. Ahn, S. Seo, Y. Kaufman, J. N. Israelachvili and J. H. Waite, *Nat. Mater.*, 2016, **15**, 407–412.
6 Y. Ma, S. Ma, Y. Wu, X. Pei, S. N. Gorb, Z. Wang, W. Liu and F. Zhou, *Adv. Mater.*, 2018, **30**, 1801595.
7 C. L. Jenkins, H. M. Siebert and J. J. Wilker, *Macromolecules*, 2017, **50**, 561–568.
8 Y. Zhao, Y. Wu, L. Wang, M. Zhang, X. Chen, M. Liu, J. Fan, J. Liu, F. Zhou and Z. Wang, *Nat. Commun.*, 2017, **8**, 2218.
9 H. Fan, J. Wang, Z. Tao, J. Huang, P. Rao, T. Kurokawa and J. P. Gong, *Nat. Commun.*, 2019, **10**, 5127.
10 H. Fan, J. Wang and J. P. Gong, *Adv. Funct. Mater.*, 2020, **30**, 2009334.
11 C. Cui, C. Fan, Y. Wu, M. Xiao, T. Wu, D. Zhang, X. Chen, B. Liu, Z. Xu, B. Qu and W. Liu, *Adv. Mater.*, 2019, **31**, 1905761.
12 L. Han, M. Wang, L. O. Prieto-López, X. Deng and J. Cui, *Adv. Funct. Mater.*, 2020, **30**, 1907064.
13 Y. Xu, Q. Liu, A. Narayanan, D. Jain, A. Dhinojwala and A. Joy, *Adv. Mater. Interfaces*, 2017, **4**, 1700506.
14 F. Pan, S. Ye, R. Wang, W. She, J. Liu, Z. Sun and W. Zhang, *Mater. Horiz.*, 2020, **7**, 2063–2070.
15 P. Rao, T. L. Sun, L. Chen, R. Takahashi, G. Shinohara, H. Guo, D. R. King, T. Kurokawa and J. P. Gong, *Adv. Mater.*, 2018, **30**, 1801884.
16 H. Jung, M. K. Kim, J. Y. Lee, S. W. Choi and J. Kim, *Adv. Funct. Mater.*, 2020, **30**, 2004407.
17 H. Yuk, T. Zhang, S. Lin, G. A. Parada and X. Zhao, *Nat. Mater.*, 2016, **15**, 190–196.
18 A. Vitale, R. Bongiovanni and B. Ameduri, *Chem. Rev.*, 2015, **115**, 8835–8866.
19 B. Améduri, B. Boutevin and G. Kostov, *Prog. Polym. Sci.*, 2001, **26**, 105–187.
20 F. Boschet and B. Ameduri, *Chem. Rev.*, 2014, **114**, 927–980.
21 A. L. Logothetis, *Prog. Polym. Sci.*, 1989, **14**, 251–296.
22 Y. Cao, H. Wu, S. I. Allec, B. M. Wong, D.-S. Nguyen and C. Wang, *Adv. Mater.*, 2018, **30**, 1804602.
23 Y. Cao, Y. J. Tan, S. Li, W. W. Lee, H. Guo, Y. Cai, C. Wang and B. C. K. Tee, *Nat. Electron.*, 2019, **2**, 75–82.
24 Y. Zhang, M. Li, B. Qin, L. Chen, Y. Liu, X. Zhang and C. Wang, *Chem. Mater.*, 2020, **32**, 6310–6317.
25 K. Fang, R. Wang, H. Zhang, L. Zhou, T. Xu, Y. Xiao, Y. Zhou, G. Gao, J. Chen, D. Liu, F. Ai and J. Fu, *ACS Appl. Mater. Interfaces*, 2020, **12**, 52307–52318.
26 L. Wang, G. Gao, Y. Zhou, T. Xu, J. Chen, R. Wang, R. Zhang and J. Fu, *ACS Appl. Mater. Interfaces*, 2019, **11**, 3506–3515.
27 X. Pei, H. Zhang, Y. Zhou, L. Zhou and J. Fu, *Mater. Horiz.*, 2020, **7**, 1872–1882.
28 H. Lai, Z. Wang, P. Wu, B. I. Chaudhary, S. S. Sengupta, J. M. Cogen and B. Li, *Ind. Eng. Chem. Res.*, 2012, **51**, 9365–9375.
29 S. Li, Y. Cong and J. Fu, *J. Mater. Chem. B*, 2021, DOI: 10.1039/D1TB00523E.
30 Z. Wang, S. Zhang, S. Zhao, H. Kang, Z. Wang, C. Xia, Y. Yu and J. Li, *Chem. Eng. J.*, 2021, **404**, 127069.
31 J. Wang, L. Wang, C. Wu, X. Pei, Y. Cong, R. Zhang and J. Fu, *ACS Appl. Mater. Interfaces*, 2020, **12**, 46816–46826.
32 J. Zhu, X. Lu, W. Zhang and X. Liu, *Macromol. Rapid Commun.*, 2020, **41**, 2000098.
33 J. Li, A. D. Celiz, J. Yang, Q. Yang, I. Wamala, W. Whyte, B. R. Seo, N. V. Vasilyev, J. J. Vlassak, Z. Suo and D. J. Mooney, *Science*, 2017, **357**, 378.
34 J. Deng, H. Yuk, J. Wu, C. E. Varela, X. Chen, E. T. Roche, C. F. Guo and X. Zhao, *Nat. Mater.*, 2021, **20**, 229–236.
35 M. G. Mazzotta, A. A. Putnam, M. A. North and J. J. Wilker, *J. Am. Chem. Soc.*, 2020, **142**, 4762–4768.
36 K. Cui, T. L. Sun, X. Liang, K. Nakajima, Y. N. Ye, L. Chen, T. Kurokawa and J. P. Gong, *Phys. Rev. Lett.*, 2018, **121**, 185501.
37 M. A. North, C. A. Del Grosso and J. J. Wilker, *ACS Appl. Mater. Interfaces*, 2017, **9**, 7866–7872.
38 Z. Wang, L. Guo, H. Xiao, H. Cong and S. Wang, *Mater. Horiz.*, 2020, **7**, 282–288.
39 A. Li, Y. Jia, S. Sun, Y. Xu, B. B. Minsky, M. A. C. Stuart, H. Cölfen, R. von Klitzing and X. Guo, *ACS Appl. Mater. Interfaces*, 2018, **10**, 10471–10479.
40 D. Lee, H. Hwang, J.-S. Kim, J. Park, D. Youn, D. Kim, J. Hahn, M. Seo and H. Lee, *ACS Appl. Mater. Interfaces*, 2020, **12**, 20933–20941.
41 X. Li, Z. Du, Z. Song, B. Li, L. Wu, Q. Liu, H. Zhang and W. Li, *Adv. Funct. Mater.*, 2018, **28**, 1800599.
42 X. Liu, Q. Zhang, L. Duan and G. Gao, *Adv. Funct. Mater.*, 2019, **29**, 1900450.
43 L. C. Tomé, A. S. L. Gouveia, C. S. R. Freire, D. Mecerreyes and I. M. Marrucho, *J. Membr. Sci.*, 2015, **486**, 40–48.

